photonics

Communication

High-Efficiency and High-Power Multijunction InGaAs/InP Photovoltaic Laser Power Converters for 1470 nm

Simon Fafard * and Denis P. Masson

Broadcom (Canada), IFPD, Ottawa, ON K1A 0R6, Canada; denis.masson@broadcom.com
* Correspondence: simon.fafard@broadcom.com

Abstract: The high-efficiency capabilities of multijunction laser power converters are demonstrated for high-power applications with an optical input of around 1470 nm. The InP-based photovoltaic power converting III-V semiconductor devices are designed here, with 10 lattice-matched subcells (PT10-InGaAs/InP), using thin InGaAs absorbing layers connected by transparent tunnel junctions. The results confirm that such long-wavelength power converter devices are capable of producing electrical output voltages greater than 4–5 V. The characteristics are compatible with common electronics requirements, and the optical input is well suited for propagation over long distances through fiber-based optical links. Conversion efficiencies of ~49% are measured at electrical outputs exceeding 7 W for an input wavelength of 1466 nm at 21 °C. The Power Converter Performance Chart has been updated with these PT10-InGaAs/InP results.

Keywords: optical power converters; laser power converters; power-over-fiber; power beaming; photovoltaic; galvanic isolation; InGaAs; InP; multijunctions semiconductor heterostructures

check for updates

Citation: Fafard, S.; Masson, D.P. High-Efficiency and High-Power Multijunction InGaAs/InP Photovoltaic Laser Power Converters for 1470 nm. *Photonics* **2022**, *9*, 438. https://doi.org/10.3390/photonics9070438

Received: 2 June 2022
Accepted: 20 June 2022
Published: 21 June 2022

1. Introduction

The developments in the past few decades in the field of applied semiconductor and optical physics served to establish a mature laser diode industry. Of particular interest, fiber-coupled multimode laser diodes with high output powers are commercially available at around 1470 nm. The low attenuation loss of optical fibers at 1470 nm is key to the implementation of these lasers and lends itself favorably to the propagation of optical power over long distances (e.g., transmission of ~95% over 1 km). In addition, in a recent perspective paper, we reviewed the developments of optical power converters (OPCs) [1–47], often also referred to as laser power converters (LPCs). The resulting Power Converter Performance Chart [41] clearly highlights that multijunction OPCs are required for obtaining not only high conversion efficiencies, but also high output powers. The research related to photovoltaic devices suggests other potential future device improvements [48–67], optical wireless power transmission applications [68–74], and system design strategies [75–78].

Many OPC developments have historically been achieved at wavelengths around 808 nm. The key benefits of this wavelength option include the good availability of laser diodes and the maturity of GaAs-based devices. More recently, ~980 nm has become an interesting wavelength option, because the laser diodes for that range can be strategic (reliability or cost) and due to the novel availability of multijunction OPCs to cover this option [37,38,41]. Another wavelength option is in the 1310 nm region, which also has interesting recent developments [30], and can benefit from the low fiber attenuation for that spectral region. Lastly, the long wavelength options of 1450–1490 nm and of the ~1550 nm region can both benefit from the lowest fiber attenuation range and from the telecommunication infrastructure [10,16,35–37,39,42,44]. Much telecommunication traffic utilizes the ~1550 nm region; the ~1470 nm option can help minimize the potential for interference between optical wireless power transmission and data transmission applications.

The Power Converter Performance Chart also revealed that more developments were necessary for multijunction OPCs based on the InGaAs/InP material system [42,44,46,47].

In the current work, we therefore present the results obtained with Broadcom's initial 10 junction InGaAs/InP prototypes, herein called PT10-InGaAs/InP, intended for operation with input from a high-power 1470 nm laser diode.

2. Materials and Methods

The InGaAs subcells lattice-matched to InP are expected to contribute ~0.5 V of output voltage each, such as based on previous single-junction measurements [41]. For this study, a PT10 design was selected (vertical multijunction with 10 subcells) in order to achieve an output voltage in the range of ~5 V. The schematic of the PT10-InGaAs/InP heterostructure is depicted in Figure 1a. This is based on the previously described Vertical Epitaxial HeteroStructure Architecture (VEHSA design) [57,58], here adapted for the lattice-matched InGaAs/InP material system. The Beer–Lambert law was used in this specific case to calculate the individual subcell's absorber thicknesses, with each subcell absorbing ~1/10 of the incident light. A ~5 V output level is common for electronic circuitry and can also provide good output power capabilities. An output level of 3.3 V is another common option for electronics and should be achievable with a seven-junction device. However, the PT10 design provides additional output voltage margins and was selected to ensure that sufficient output voltage can be maintained under higher operating temperatures. For a GaAs-based system, we have demonstrated that the output voltage scales linearly up to PT30 devices with 30 subcells. Similarly, we would expect devices with more than 10 InGaAs subcells to readily be realized, although a PT10 design is expected to meet the most common output voltage requirements and was the focus of the present study.

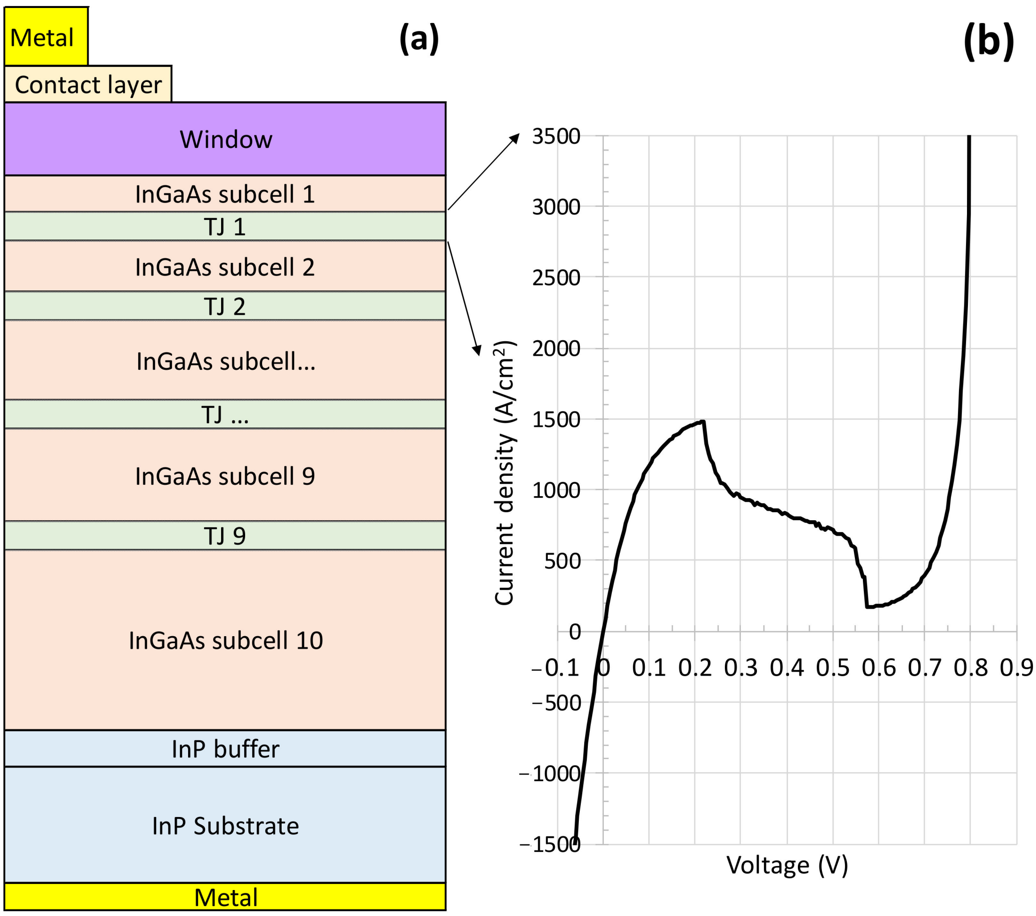

Figure 1. Schematic of the PT10-InGaAs/InP Vertical Epitaxial HeteroStructure Architecture (VEHSA design) devices prepared with 10 InGaAs subcells in (**a**), and I–V characteristics of the tunnel junction (TJ) measured from a single TJ grown separately in a truncated structure in (**b**).

The photovoltaic vertical multijunction structure was built for operation with optical input from a powerful laser source emitting in a spectral range peaking around 1470 nm. It is designed with 10 thin (optically transparent) photovoltaic semiconductor subcells interconnected with tunnel junctions, labelled TJi in Figure 1a. Each individual subcell comprises an n-type emitter and a p-type base. The TJs are made to be transparent to the input beam, utilizing an InGaAlAsP alloy lattice-matched to InP with a bandgap of about 1 eV. The TJ's current–voltage (I–V) characteristics have been verified on truncated structures (i.e., isolated TJ structures) grown under comparable conditions. For example, Figure 1b shows the I–V curve of such an isolated TJ with its negative differential resistance (NRD) region (here, 0.2 V < V < 0.6 V), confirming the tunnel current characteristics. Of particular interest is the elevated peak tunneling current capabilities (here, ~1500 A/cm^2) and the related very low voltage drops under the normal multijunction OPC operations (usually with peak current densities of J < 100 A/cm^2).

The epitaxial layers were grown using commercial production Aixtron Metal Organic Chemical Vapor Deposition (MOCVD) reactors. The total thickness of all the emitter and base layers from the different subcells is such that the impinging optical beam is almost completely absorbed. For the InP material system, an interesting design variation consists of reducing the absorber thicknesses of the subcells and using light reflected from the back side. The InP substrate is transparent to the input light and to the InGaAs luminescence, therefore allowing the light reflected [8] from the back side of the device to be recycled [79–82]. Nevertheless, as described previously [41,58], to realize the required photocurrent matching condition, the structure usually has increasing subcell thicknesses from the top subcell (thinnest) toward the bottom subcell (thickest).

The device fabrication included standard blanket back-metallization (SnZnIn, PdZn-PdAu, or PdZnPtAu contacts) [83], front ohmic contacts (Pd/Ge/Ti/Pd/Ag/Au or In), and antireflection coatings (ARC) constructed from multiple layers of SiO_2 and TiO_2. The ARC was measured to reduce the reflectivity (R) of the incident beam to R < 2% for the spectral range of interest.

A fiber-coupled laser diode manufactured by BWT was used [84]. Its optical output power reaches a maximum of 14.5 W at an operating current of 6.3 A at a voltage bias of ~9.4 V. It had a numerical aperture of NA ~0.22, using a multi-mode fiber core diameter of 400 µm and cladding of 440 µm. It was equipped with an integrated red aiming beam, which was used to align the ~1470 nm beam. For the I–V measurements, the tip of the fiber-coupled laser was positioned to form a circular spot with a radius of about 2.6 mm from the diverging laser beam. The spot covered roughly 50% of the sample's central area.

The I–V characteristics were acquired using a Keithley 2601B source-meter. The data were obtained at a temperature of ~21 °C and the measurements were made to avoid significant chip heating.

3. Results

The key result measured with the PT10-InGaAs/InP from this study is added as a data point (45) in Figure 2, which shows the updated power converter performance chart built from the results published in the literature [41]. Detailed results from the PT10-InGaAs/InP OPCs are then presented below.

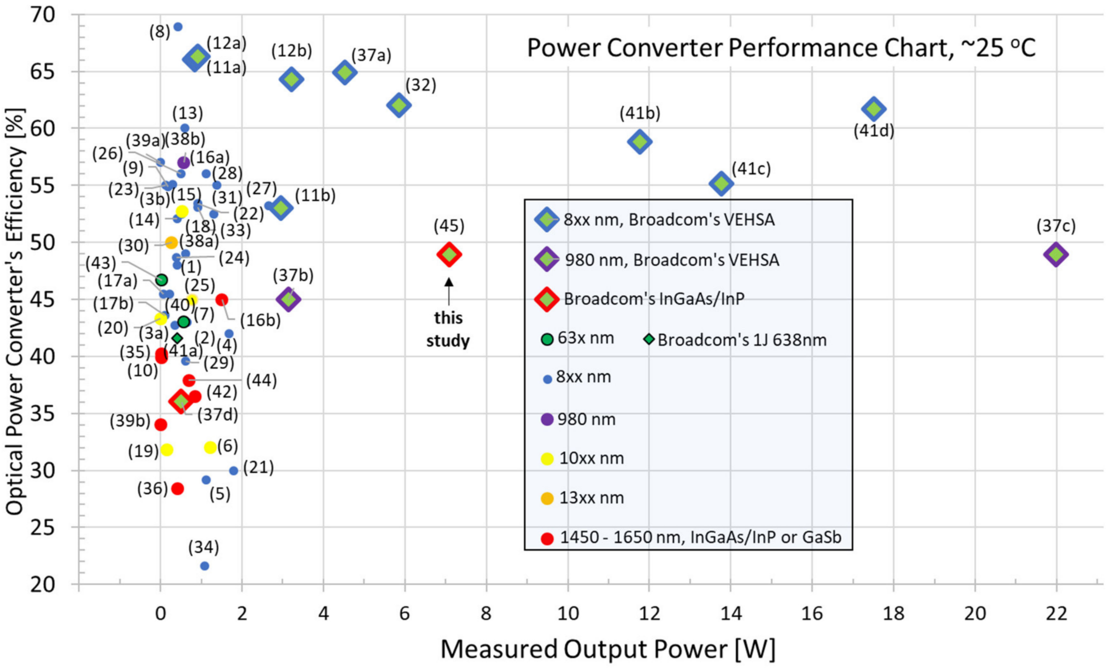

Figure 2. Survey of the measured performance for monolithic power converter devices at the indicated laser wavelengths. Single junction, vertical multijunction, and planar segmented ("pizza" configuration) device reports are included (module results are not included here). Updated from Fafard, S. and Masson, D.P., J. Applied Physics 130, 160901 (2021). Copyright 2021 Author(s), licensed under a Creative Commons Attribution (CC BY) license [41]: (1) 1J-GaAs (2018) Jomen et al. [1], (2) 1J-InGaP (2021) Komuro et al. [2], (3a) Pizza-6 (2009) Schubert et al. [3], (3b) Pizza-4 (2009) Schubert et al. [3], (4) 6J-GaAs (2016) Zhao et al. [4], (5) 6J-GaAs (2017) Sun et al. [5], (6) 3J-InGaAsP (2020) Yin et al. [6], (7) 4J (2018) Huang et al. [7], (8) Back Mirror (2021) Helmers et al. [8], (9) 1J-GaAs (2008) Oliva et al. [9], (10) 1J-InGaAs (2013) Mukherjee et al. [10], (11a) PT5 (2016) Fafard et al. [11], (11b) PT12/8/6 (2016) Fafard et al. [11], (12a) PT5 (2016) Fafard et al. [12], (12b) PT12/20 (2016) Fafard et al. [12], (13) 1J-GaAs (2016) Kalyuzhnyy et al. [13], (14) 1J-GaAs (1992) Olsen et al. [14], (15) 2J-GaAs (2007) Krut et al. [15], (16a) 1J-GaAs (2003) Andreev et al. [16], (16b) 1J-GaSb (2003) Andreev et al. [16], (17a) Pizza-4 (2003) Peña et al. [17], (17b) Pizza-6 (2003) Peña et al. [17], (18) InGaAs (2020) Kalyuzhnyy et al. [18], (19) InGaAs-Meta (2019) Kim et al. [19], (20) 1J-InGaAsP (1981) Law et al. [20], (21) 1J-GaAs (2019) Panchak et al. [21], (22) Pizza-6 (2008) Bett et al. [22], (23) Pizza-6 (1996) Fahrenbruch et al. [23], (24) 1J-GaAs (1996) Fave et al. [24], (25) 1J-Si (1992) Green et al. [25], (26) 1J-GaAs (2016) Höhn et al. [26], (27) 1J-GaAs-R_{mpp} = 0.38 Ohm, (2015) Shan et al. [27], (28) 1J-GaAs (2018) Khvostikov et al. [28], (29) 1J-GaAs (2017) Khvostikov et al. [29], (30) 1J-InGaAsP (2020) Helmers et al. [30], (31) 1J-GaAs (2019) Zhao et al. [31], (32) PT6 (2017) York et al. [32], (33) 6J-GaAs (2018) Huang et al. [33], (34) 6J-GaAs in TO (2017) Ding et al. [34], (35) 1J-InGaAs (2014) Jarvis et al. [35], (36) 1J-GaSb (2019) Khvostikov et al. [36], (37a) PT6-GaAs (2021) Fafard et al. [37], (37b) PT6-InGaAs (2021) Fafard et al. [37], (37c) PT6-InGaAs (2021) Fafard et al. [37], (37d) 1J-InGaAs (2021) Fafard et al. [37], (38a) 3J-GaAs (2021) Keller et al. [38], (38b) 5J-InGaAs (2021) Keller et al. [38], (39a) 1J-GaAs (1997) Wojtczuk et al. [39], (39b) 1J-InGaAs (1997) Wojtczuk et al. [39], (40) Pizza-4 (2010) Eggert et al. [40], (41a) 1J-InGaP (2021) Fafard et al. [41], (41b) PT12 (2021) Fafard et al. [41], (41c) PT5 (2021) Fafard et al. [41], (41d) PT6 (2021) Fafard et al. [41], (42) 8J-InGaAs/InP (2021) Wang et al. [42], (43) 1J-InGaP (2022) Kurooka et al. [43], (44) 1J-InGaAs (2022) Helmers et al. [44], (45) PT10-InGaAs/InP (2022) Fafard and Masson (this study).

The measured I–V curves are shown in Figure 3 for various optical input powers between P_{in} = 2.5 W and P_{in} = 14.5 W. The dashed (pink) curve in Figure 3 is an ideal diode model fitted with the 5.0 W data. A good fit is obtained here, using 10 diodes all with the same ideality factor of n = 1.05 and the same photocurrent ratio corresponding to a quantum efficiency of EQE = 93%. The fit accurately reproduces the data when the overall series resistance is set at 0.00 Ohm. Furthermore, the dark I–V measurements (not shown) also support that any residual series resistance should be smaller than a fraction of 1 Ohm. It can also be deduced that the current-matching in the individual 10 subcells is high for a spectral input at a wavelength near 1466 nm. The latter is evidenced by the high EQE value measured at ~93% and the flatness of the horizontal part of the I–V curves.

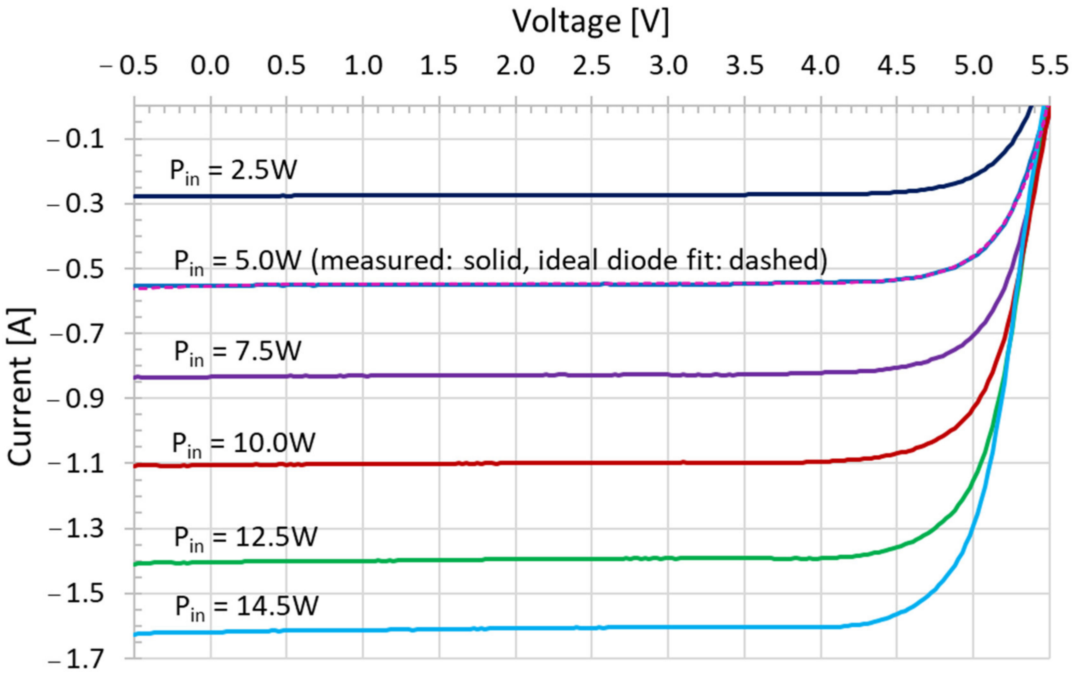

Figure 3. Measured I–V properties at 21 °C for a PT10-InGaAs/InP OPC operating with a laser peaking at 1466 nm, for input powers between 2.5 W and 14.5 W. At 14.5 W of input power, an efficiency of Eff = 48.9% is obtained with a V_{oc} of 5.46 V. The output power (P_{mpp}) reaches 7.09 W with V_{mpp} = 4.675 V and I_{mpp} = 1.517 A. The 5.0 W curve is also fitted with a 10J ideal diode model (pink dashed line).

The key characteristics of the I–V curves in Figure 3 are analyzed in more detail in Figure 4, which shows the input power dependence of key parameters. Figure 4a shows that the output power P_{mpp} has a measured slope efficiency of Eff $\sim$ 49%, with negligible deviations from linear regression for optical input powers up to 14.5 W. Here, the input power was limited by the laser's maximum output power. Provided adequate heatsinking is available to the device; we expect that it would be possible to use higher input powers without damaging the photovoltaic laser power converter.

The output voltage is shown in Figure 4b. The open-circuit voltage (V_{oc}) reaches a maximum value of 5.508 V, while the maximum power point voltage (V_{mpp}) is then 4.75 V. It corresponds to an average voltage of 0.551 V per subcell, yielding a bandgap voltage offset value of W_{oc} = 0.187 V, where $W_{oc} = (Eg/q) - V_{oc}$ with Eg being the bandgap energy (here, InGaAs lattice-matched to InP) and q is the electronic charge. The W_{oc} value obtained with the PT10-InGaAs/InP is therefore very similar to that measured for the GaAs OPCs at W_{oc} = 0.181 V [41].

The external quantum efficiency (EQE) is shown in Figure 4c. At a voltage bias of 4 V, an EQE of 92% is obtained for input powers up to ~5 W. As the input power is increased, the EQE at 4 V increases slightly, up to 93.5% at 14.5 W. The increased EQE value at higher optical intensities could be caused by a higher photon recycling, giving a better current-matching at higher input powers [79–82].

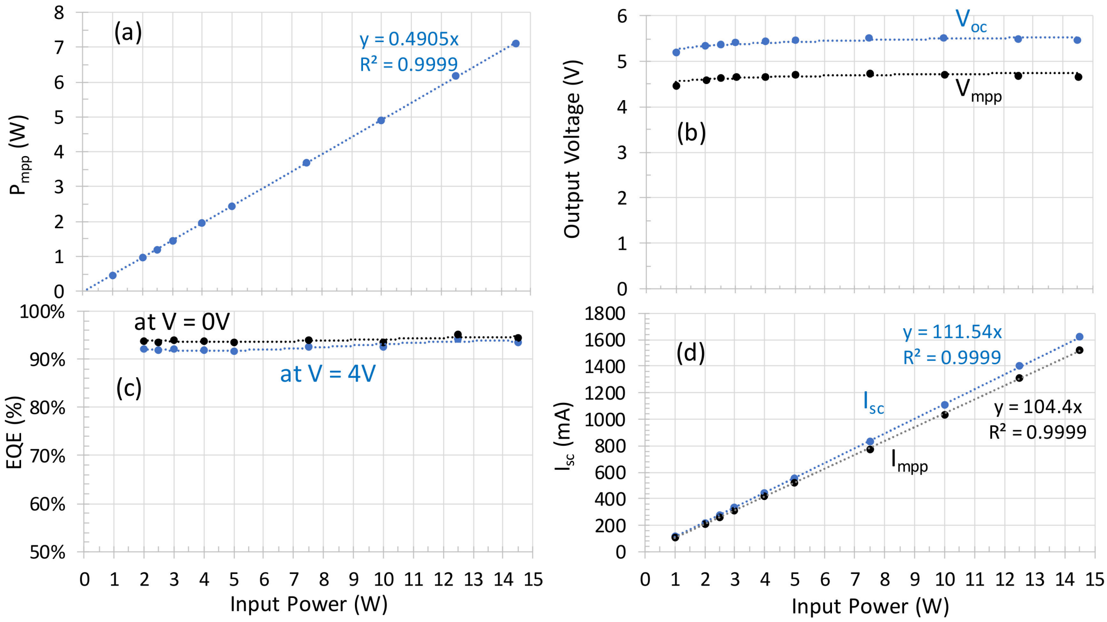

Figure 4. The PT10-InGaAs/InP's input power dependence with an incident laser beam peaking at 1466 nm at 21 °C. The electrical output power, P_{mpp}, is shown in (**a**), the output voltage: open-circuit voltage (V_{oc}) and maximum power point voltage (V_{mpp}) are shown in (**b**), the external quantum efficiency (EQE) is shown in (**c**), and the output current, short-circuit current (I_{sc}) and maximum power point current (I_{mpp}), are shown in (**d**). The values of the linear regressions are indicated in the plots.

The output current is shown in Figure 4d. The short-circuit current (I_{sc}) yields a responsivity of 1.115 A/W (taking into account the 10 junctions of the PT10). For a wavelength of 1466 nm, this corresponds to an EQE of 94.3%. The maximum power point current (I_{mpp}) is measured to have a responsivity of 1.044 A/W, corresponding to an EQE of 88.3%.

4. Discussions

As can be visualized from Figure 2, the PT10-InGaAs/InP performance in Figures 3 and 4 is a drastic improvement from the results previously obtained with InGaAs/InP power converters. Record efficiencies are obtained for unprecedented output power capabilities at such long wavelengths. For example, the optimal load ($R_{mpp} = V_{mpp}/I_{mpp}$) of a PT10 is 100 times larger than that from the corresponding single junction; the impact is best observed in Figure 5. To exemplify the benefits of the multijunction devices, results were obtained with various OPC designs in different material systems. We include data from single junctions ("PT1") to 12-junction GaAs devices ("PT12-GaAs"). Here, the PT12-GaAs has the highest output power capabilities, as can be observed from Figure 5. Our study also includes the data acquired with four OPC designs obtained using the InGaAs/InP material system, "PTN-InGaAs/InP", with N = 1, 2, 3, and 10, corresponding to the number of InGaAs subcells. The output voltage of the InGaAs/InP multijunction devices increases by increments of V_{mpp} ~0.475 V per subcell (as previously shown in Figure 4b). This makes these OPC devices more suitable for operation at higher-input powers. The PT2-InGaAs/InP has an output characteristic similar to the single-junction GaAs device ("PT1-GaAs"), and can already operate at significantly higher input power than a single junction InGaAs ("PT1-976") device, optimized for input at ~976 nm. The PT10-InGaAs/InP at ~1470 nm has an output characteristic between that of a four-junction GaAs device ("PT4-GaAs") and that of a six-junction GaAs device ("PT6-GaAs") device, both optimized for input at ~808 nm.

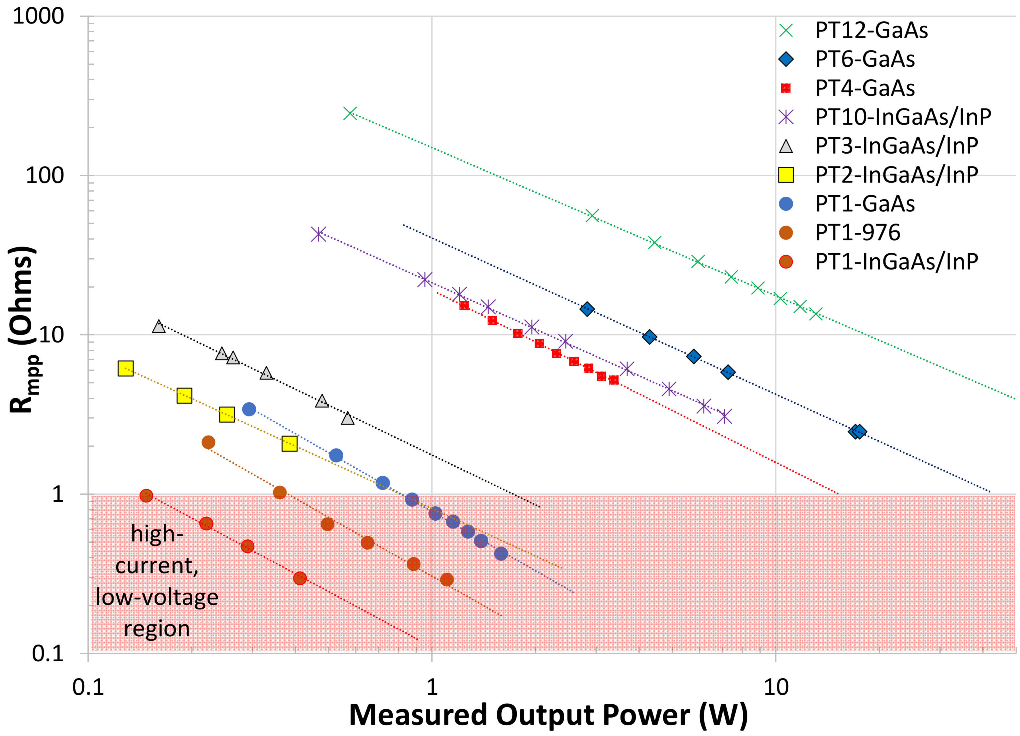

Figure 5. The measured optimal load ($R_{mpp} = V_{mpp}/I_{mpp}$) as a function of the output power obtained with various OPC designs. As indicated in the caption, results are measured for the following OPC designs: single junctions from the material systems of InGaAs/InP ("PT1-InGaAs/InP") at ~1470 nm [37], of InGaAs/GaAs ("PT1-976") at ~976 nm [37], and of GaAs ("PT1-GaAs") at ~808 nm [37,57]; from multijunctions from the InGaAs/InP material system, "PTN-InGaAs/InP", with N = 2, 3, and 10, corresponding to the number of InGaAs subcells [this study]; and from multijunctions from the GaAs material system, "PTN-GaAs", with N = 4, 6, and 12, corresponding to the number of GaAs subcells [37,41]. The area of low voltage and high current is shown in pink and is less desirable for practical applications.

Figure 5 clearly demonstrates that for achieving higher OPC output powers while maintaining high efficiencies, it is necessary to increase the device output voltage; otherwise, the optimal load collapses to unusable small values. The latter is illustrated with the pink region of Figure 5, which corresponds to the situation when the ratio of V_{mpp} over I_{mpp} becomes smaller than ~1 Ohm. In these cases, it becomes very problematic to maintain high conversion efficiencies.

5. Conclusions

In conclusion, the vertical multijunction VEHSA strategy has been proven very effective at trading photocurrents to increase the operating voltage in long-wavelength OPCs. Conversion efficiencies of Eff ~49% have been measured at electrical outputs exceeding 7 W for an input wavelength of 1466 nm, with the PT10-InGaAs/InP device giving a V_{oc} of 5.46 V. An ideality factor of n ~1.05 was found for this material system. The 4 V EQE, at high optical input powers, was measured to be ~93.5%, combined with a residual reflectivity of R < 2%. In future iterations, the EQE and IQE could therefore be further optimized by potentially up to 2% to 4%. The W_{oc} value was measured to be ~187 mV with a lattice-matched InGaAs absorber. The use of an AlInGaAsP alloy for the absorber with a slightly higher bandgap (e.g., 0.8 eV) could potentially improve the V_{mpp} values by >50 mV per subcells. Such additional optimizations could definitely lift the conversion efficiency of long-wavelength InP-based power converters above 50%.

Author Contributions: Conceptualization, S.F. and D.P.M.; methodology, S.F. and D.P.M.; software, S.F. and D.P.M.; validation, S.F. and D.P.M.; formal analysis, S.F. and D.P.M.; investigation, S.F. and D.P.M.; data curation, S.F. and D.P.M.; writing—original draft preparation, S.F.; writing—review and editing, S.F. and D.P.M.; visualization, S.F.; project administration, S.F. and D.P.M.; funding acquisition, S.F. and D.P.M. All authors have read and agreed to the published version of the manuscript.

Funding: This research received no external funding.

Institutional Review Board Statement: Not applicable.

Informed Consent Statement: Not applicable.

Data Availability Statement: The data that support the findings of this study are available from the corresponding author upon reasonable request.

Conflicts of Interest: The authors declare no particular conflicts of interest, but it should be noted that the authors are employed by Broadcom, a company that manufactures and sells semiconductor components, including power converter devices.

References

1. Jomen, R.; Tanaka, F.; Akiba, T.; Ikeda, M.; Kiryu, K.; Matsushita, M.; Maenaka, H.; Dai, P.; Lu, S.; Uchida, S. Conversion efficiencies of single-junction III–V solar cells based on InGaP, GaAs, InGaAsP, and InGaAs for laser wireless power transmission. *Jpn. J. Appl. Phys.* **2018**, *57*, 08RD12. [CrossRef]
2. Komuro, Y.; Honda, S.; Kurooka, K.; Warigaya, R.; Tanaka, F.; Uchida, S. A 43.0% efficient GaInP photonic power converter with a distributed Bragg reflector under high-power 638 nm laser irradiation of 17 Wcm-2. *Appl. Phys. Express* **2021**, *14*, 052002. [CrossRef]
3. Schubert, J.; Oliva, E.; Dimroth, F.; Guter, W.; Loeckenhoff, R.; Bett, A.W. High-Voltage GaAs Photovoltaic Laser Power Converters. *IEEE Trans. Electron Devices* **2009**, *56*, 170–175. [CrossRef]
4. Zhao, Y.; Sun, Y.; He, Y.; Yu, S.; Dong, J. Design and fabrication of six-volt vertically-stacked GaAs photovoltaic power converter. *Sci. Rep.* **2016**, *6*, 38044. [CrossRef]
5. Sun, Y.-R.; Dong, J.-R.; He, Y.; Zhao, Y.-M.; Yu, S.-Z.; Xue, J.-P.; Xue, C.; Wang, J.; Lu, Y.-Q.; Ding, Y.-W. A six-junction GaAs laser power converter with different sizes of active aperture. *Optoelectron. Lett.* **2017**, *13*, 21–24. [CrossRef]
6. Yin, J.; Sun, Y.; Yu, S.; Zhao, Y.; Li, R.; Dong, J. 1064 nm InGaAsP multi-junction laser power converters. *J. Semicond.* **2020**, *41*, 062303. [CrossRef]
7. Huang, J.; Sun, Y.; Zhao, Y.; Yu, S.; Dong, J.; Xue, J.; Xue, C.; Wang, J.; Lu, Y.; Ding, Y. Four-junction AlGaAs/GaAs laser power converter. *J. Semicond.* **2018**, *39*, 044003. [CrossRef]
8. Helmers, H.; Lopez, E.; Höhn, O.; Lackner, D.; Schön, J.; Schauerte, M.; Schachtner, M.; Dimroth, F.; Bett, A.W. 68.9% Efficient GaAs-Based Photonic Power Conversion Enabled by Photon Recycling and Optical Resonance. *Phys. Status Solidi (RRL) Rapid Res. Lett.* **2021**, *15*, 2100113. [CrossRef]
9. Oliva, E.; Dimroth, F.; Bett, A.W. GaAs converters for high power densities of laser illumination. *Prog. Photovol. Res. Appl.* **2008**, *16*, 289–295. [CrossRef]
10. Mukherjee, J.; Jarvis, S.; Perren, M.; Sweeney, S.J. Efficiency limits of laser power converters for optical power transfer applications. *J. Phys. D Appl. Phys.* **2013**, *46*, 264006. [CrossRef]
11. Fafard, S.; York, M.C.A.; Proulx, F.; Valdivia, C.E.; Wilkins, M.M.; Arès, R.; Aimez, V.; Hinzer, K.; Masson, D.P. Ultrahigh efficiencies in vertical epitaxial heterostructure architectures. *Appl. Phys. Lett.* **2016**, *108*, 071101. [CrossRef]
12. Fafard, S.; Proulx, F.; York, M.C.A.; Richard, L.S.; Provost, P.O.; Arès, R.; Aimez, V.; Masson, D.P. High-photovoltage GaAs vertical epitaxial monolithic heterostructures with 20 thin p/n junctions and a conversion efficiency of 60%. *Appl. Phys. Lett.* **2016**, *109*, 131107. [CrossRef]
13. Khvostikov, V.P.; Kalyuzhnyy, N.A.; Mintairov, S.; Sorokina, S.V.; Potapovich, N.S.; Emelyanov, V.M.; Timoshina, N.K.; Andreev, V.M. Photovoltaic laser-power converter based on AlGaAs/GaAs heterostructures. *Semiconductors* **2016**, *50*, 1220–1224. [CrossRef]
14. Olsen, L.C.; Huber, D.A.; Dunham, G.; Addis, F.W. High efficiency monochromatic GaAs solar cells. In Proceedings of the Conference Record of the Twenty-Second IEEE Photovoltaic Specialists Conference-1991, Las Vegas, NV, USA, 7–11 October 1991; pp. 419–424.
15. Krut, D.; Sudharsanan, R.; Isshiki, T.; King, R.; Karam, N. A 53% high efficiency gaas vertically integrated multi-junction laser power converter. In Proceedings of the 2007 65th Annual Device Research Conference, South Bend, IN, USA, 18–20 June 2007; pp. 123–124.
16. Andreev, V.; Khvostikov, V.; Kalinovsky, V.; Lantratov, V.; Grilikhes, V.; Rumyantsev, V.; Shvarts, M.; Fokanov, V.; Pavlov, A. High current density GaAs and GaSb photovoltaic cells for laser power beaming. In Proceedings of the 3rd World Conference on Photovoltaic Energy Conversion, Osaka, Japan, 11–18 May 2003; Volume 1, pp. 761–764.
17. Peña, R.; Algora, C.; Anton, I. GaAs multiple photovoltaic converters with an efficiency of 45% for monochromatic illumination. In Proceedings of the 3rd World Conference on Photovoltaic Energy Conversion, Osaka, Japan, 11–18 May 2003; pp. 228–231.

18. Kalyuzhnyy, N.A.; Emelyanov, V.; Mintairov, S.A.; Shvarts, M.Z. InGaAs metamorphic laser (λ = 1064 nm) power converters with over 44% efficiency. *AIP Conf. Proc.* **2018**, *2012*, 110002.
19. Kim, Y.; Shin, H.-B.; Lee, W.-H.; Jung, S.H.; Kim, C.Z.; Kim, H.; Lee, Y.T.; Kang, H.K. 1080 nm InGaAs laser power converters grown by MOCVD using InAlGaAs metamorphic buffer layers. *Sol. Energy Mater. Sol. Cells* **2019**, *200*, 109984. [CrossRef]
20. Law, H.D.; Ng, W.W.; Nakano, K.; Dapkus, P.D.; Stone, D.R. High Efficiency InGaAsP Photovoltaic Power Converter. *IEEE Electron Device Lett.* **1981**, *2*, 26–27. [CrossRef]
21. Panchak, A.N.; Pokrovskiy, P.V.; Malevskiy, D.A.; Larionov, V.R.; Shvarts, M.Z. High-Efficiency Conversion of High-Power-Density Laser Radiation. *Tech. Phys. Lett.* **2019**, *45*, 24–26. [CrossRef]
22. Bett, A.W.; Dimroth, F.; Lockenhoff, R.; Oliva, E.; Schubert, J. III–V solar cells under monochromatic illumination. In Proceedings of the Conference Record of the 2008 33rd IEEE Photovoltaic Specialists Conference, San Diego, CA, USA, 11–16 May 2008; p. 4922910.
23. Fahrenbruch, A.L.; Lopez-Otero, A.; Werthen, J.G.; Wu, T.C. GaAs- and InAlGaAs-based concentrator-type cells for conversion of power transmitted by optical fibers. In Proceedings of the Conference Record of the Twenty Fifth IEEE Photovoltaic Specialists Conference, Washington, DC, USA, 13–17 May 1996; pp. 117–120.
24. Fave, A.; Kaminski, A.; Gavand, M.; Mayet, L.; Laugier, A. GaAs converter for high power laser diode. In Proceedings of the Conference Record of the IEEE Photovoltaic Specialists Conference, Washington, DC, USA, 13–17 May 1996; pp. 101–104.
25. Green, M.; Zhao, J.; Wang, A.; Wenham, S. 45% efficient silicon photovoltaic cell under monochromatic light. *IEEE Electron Device Lett.* **1992**, *13*, 317–318. [CrossRef]
26. Höhn, O.; Walker, A.W.; Bett, A.W.; Helmers, H. Optimal laser wavelength for efficient laser power converter operation over temperature. *Appl. Phys. Lett.* **2016**, *108*, 241104. [CrossRef]
27. Shan, T.; Qi, X. Design and optimization of GaAs photovoltaic converter for laser power beaming. *Infrared Phys. Technol.* **2015**, *71*, 144–150. [CrossRef]
28. Khvostikov, V.P.; Sorokina, S.V.; Potapovich, N.S.; Khvostikova, O.A.; Timoshina, N.K.; Shvarts, M.Z. Modification of Photovoltaic Laser-Power (λ = 808 nm) Converters Grown by LPE. *Semiconductors* **2018**, *52*, 366–370. [CrossRef]
29. VKhvostikov, P.; Sorokina, S.V.; Potapovich, N.S.; Khvostikova, O.A.; Timoshina, N.K. Laser (λ = 809 nm) power converter based on GaAs. *Semiconductors* **2017**, *51*, 645. [CrossRef]
30. Helmers, H.; Franke, A.; Lackner, D.; Höhn, O.; Predan, F.; Dimroth, F. 51% Efficient Photonic Power Converters for O-Band Wavelengths around 1310 nm. In Proceedings of the Conference Record of the 2020 47th IEEE Photovoltaic Specialists Conference, Calgary, AB, Canada, 15 June–21 August 2020; pp. 2471–2474.
31. Zhao, Y.; Liang, P.; Ren, H.; Han, P. Enhanced efficiency in 808 nm GaAs laser power converters via gradient doping. *AIP Adv.* **2019**, *9*, 105206. [CrossRef]
32. York, M.C.A.; Fafard, S. High efficiency phototransducers based on a novel vertical epitaxial heterostructure architecture (VEHSA) with thin p/n junctions. *J. Phys. D: Appl. Phys.* **2017**, *50*, 173003. [CrossRef]
33. Huang, J.; Sun, Y.; Zhao, Y.; Yu, S.; Li, K.; Dong, J.; Xue, J.; Xue, C.; Ye, Y. Characterizations of high-voltage vertically-stacked GaAs laser power converter. *J. Semicond.* **2018**, *39*, 094006. [CrossRef]
34. Ding, Y.; Li, Q.; Lu, Y.; Wang, J. TO-packaged, multi-junction GaAs laser power converter with output electric power over 1 W. In Proceedings of the 2017 Conference on Lasers and Electro-Optics Pacific Rim (CLEO-PR), Singapore, 31 July–4 August 2017; pp. 1–3.
35. Jarvis, S.D.; Mukherjee, J.; Perren, M.; Sweeney, S.J. Development and characterisation of laser power converters for optical power transfer applications. *IET Optoelectron.* **2014**, *8*, 64–70. [CrossRef]
36. Khvostikov, V.P.; Sorokina, S.V.; Khvostikova, O.A.; Potapovich, N.S.; Malevskaya, A.V.; Nakhimovich, M.V.; Shvarts, M.Z. GaSb photovoltaic cells for laser power conversion. *AIP Conf. Proc.* **2019**, *2149*, 050007.
37. Fafard, S.; Masson, D.; Werthen, J.-G.; Liu, J.; Wu, T.-C.; Hundsberger, C.; Schwarzfischer, M.; Steinle, G.; Gaertner, C.; Piemonte, C.; et al. Power and Spectral Range Characteristics for Optical Power Converters. *Energies* **2021**, *14*, 4395. [CrossRef]
38. Keller, G. GaAs multi-junction laser power converters at AZUR SPACE: Current status and development activities. In Proceedings of the 1st Optical Wireless Fiber Power Transmission Conference, Yokohama, Japan, 23–25 April 2019; pp. 11–12.
39. Wojtczuk, S.J. Long-wavelength laser power converters for optical fibers. In Proceedings of the Conference Record of the Twenty Sixth IEEE Photovoltaic Specialists Conference-1997, Anaheim, CA, USA, 29 September–3 October 1997; pp. 971–974.
40. Eggert, N.; Rusack, R.; Mans, J. Evaluation of photonic power converters. *J. Instrum.* **2010**, *5*, T02001. [CrossRef]
41. Fafard, S.; Masson, D.P. Perspective on photovoltaic optical power converters. *J. Appl. Phys.* **2021**, *130*, 160901. [CrossRef]
42. Wang, A.-C.; Sun, Y.-R.; Yu, S.-Z.; Yin, J.-J.; Zhang, W.; Wang, J.-S.; Fu, Q.-X.; Han, Y.-H.; Qin, J.; Dong, J.-R. Characteristics of 1520 nm InGaAs multijunction laser power converters. *Appl. Phys. Lett.* **2021**, *119*, 243902. [CrossRef]
43. Kurooka, K.; Honda, T.; Komazawa, Y.; Warigaya, R.; Uchida, S. A 46.7% efficient GaInP photonic power converter under high-power 638 nm laser uniform irradiation of 1.5 W cm^{-2}. *Appl. Phys. Express* **2022**, *15*, 062003. [CrossRef]
44. Helmers, H.; Hohn, O.; Tibbits, T.; Schauerte, M.; Amin, H.M.N.; Lackner, D. Unlocking 1550 nm laser power conversion by InGaAs single- and multiple-junction PV cells. In Proceedings of the PVSC 2022—IEEE 49th PVSC 2016—IEEE 43rd Photovoltaic Specialists Conference, Philadelphia, PA, USA, 5–9 June 2022.
45. Fafard, S.; York, M.C.A.; Proulx, F.; Wilkins, M.; Valdivia, C.E.; Bajcsy, M.; Ban, D.; Arès, R.; Aimez, V.; Hinzer, K.; et al. Ultra-efficient N-junction photovoltaic cells with Voc > 14 V at high optical input powers. In Proceedings of the 2016 IEEE 43rd Photovoltaic Specialists Conference (PVSC), Portland, OR, USA, 5–10 June 2016; p. 2374.

46. Fafard, S.; Masson, D.; Werthen, J.-G.; Liu, J.; Wu, T.C.; Hundsberger, C.; Schwarzfischer, M.; Steinle, G.; Gaertner, C.; Piemonte, C.; et al. High-Efficiency Photovoltaic Power Converters and Application to Optical Power Transmission. In Proceedings of the 26th Microoptics Conference (MOC), Hamamatsu, Japan, 26–29 September 2021; pp. 1–2.
47. Fafard, S.; Masson, D.; Werthen, J.-G.; Liu, J.; Wu, T.C.; Hundsberger, C.; Schwarzfischer, M.; Steinle, G.; Gaertner, C.; Piemonte, C.; et al. High performance laser power converters and applications. In Proceedings of the Technical Digest of The 4th Optical Wireless and Fiber Power Transmission Conference (OWPT2022), Yokohama, Japan, 18–21 April 2022.
48. Lozano, J.F.; Seoane, N.; Comesaña, E.; Almonacid, F.; Fernández, E.F.; García-Loureiro, A. Laser Power Converter Architectures Based on 3C-SiC with Efficiencies >80%. *Sol. RRL* **2022**, 2101077. [CrossRef]
49. Fernández, E.F.; García-Loureiro, A.; Seoane, N.; Almonacid, F. Band-gap material selection for remote high-power laser transmission. *Sol. Energy Mat. Sol. Cells* **2022**, *235*, 111483. [CrossRef]
50. France, R.M.; Buencuerpo, J.; Bradsby, M.; Geisz, J.F.; Sun, Y.; Dhingra, P.; Lee, M.L.; Steiner, M.A. Graded buffer Bragg reflectors with high reflectivity and transparency for metamorphic optoelectronics. *J. Appl. Phys.* **2021**, *129*, 173102. [CrossRef]
51. Beattie, M.N.; Valdivia, C.E.; Wilkins, M.M.; Zamiri, M.; Kaller, K.L.C.; Tam, M.C.; Kim, H.S.; Krich, J.J.; Wasilewski, Z.R.; Hinzer, K. High current density tunnel diodes for multi-junction photovoltaic devices on InP substrates. *Appl. Phys. Lett.* **2021**, *118*, 062101. [CrossRef]
52. Wagner, L.; Reichmuth, S.K.; Philipps, S.P.; Oliva, E.; Bett, A.W.; Helmers, H. Integrated series/parallel connection for photovoltaic laser power converters with optimized current matching. *Prog. Photovolt. Res. Appl.* **2020**, *29*, 172. [CrossRef]
53. Panchak, A.; Khvostikov, V.; Pokrovskiy, P. AlGaAs gradient waveguides for vertical p/n junction GaAs laser power con-verters. *Opt. Laser Technol.* **2021**, *136*, 106735. [CrossRef]
54. Lin, M.; Sha, W.E.I.; Zhong, W.; Xu, D. Intrinsic losses in photovoltaic laser power converters. *Appl. Phys. Lett.* **2021**, *118*, 104103. [CrossRef]
55. Zhao, Y.; Li, S.; Ren, H.; Li, S.; Han, P. Energy band adjustment of 808 nm GaAs laser power converters via gradient doping. *J. Semicond.* **2021**, *42*, 032701. [CrossRef]
56. Nouri, N.; Valdivia, C.E.; Beattie, M.N.; Zamiri, M.S.; Krich, J.J.; Hinzer, K. Ultrathin monochromatic photonic power converters with nanostructured back mirror for light trapping of 1310-nm laser illumination. *SPIE* **2021**, *11681*, 116810X. [CrossRef]
57. Masson, D.; Proulx, F.; Fafard, S. Pushing the limits of concentrated photovoltaic solar cell tunnel junctions in novel high-efficiency GaAs phototransducers based on a vertical epitaxial heterostructure architecture. *Prog. Photovolt. Res. Appl.* **2015**, *23*, 1687–1696. [CrossRef]
58. Fafard, S.; Masson, D.P. Transducer to Convert Optical Energy to Electrical Energy. U.S. Patent 9,673,343, 6 June 2017.
59. Wulf, J.; Oliva, E.; Mikolasch, G.; Bartsch, J.; Dimroth, F.; Helmers, H. Thin film GaAs solar cell enabled by direct rear side plating and patterned epitaxial lift-off. In Proceedings of the 2021 IEEE 48th Photovoltaic Specialists Conference (PVSC), Fort Lauderdale, FL, USA, 20–25 June 2021; p. 1931.
60. Helmers, H.; Lopez, E.; Hohn, O.; Lackner, D.; Schon, J.; Schauerte, M.; Schachtner, M.; Dimroth, F.; Bett, A.W. Pushing the Boundaries of Photovoltaic Light to Electricity Conversion: A GaAs Based Photonic Power Converter with 68.9% Efficiency. In Proceedings of the 2021 IEEE 48th Photovoltaic Specialists Conference (PVSC), Fort Lauderdale, FL, USA, 20–25 June 2021; pp. 2286–2289.
61. Schauerte, M.; Höhn, O.; Wierzkowski, T.; Keller, G.; Helmers, H. 4-Junction GaAs Based Thin Film Photonic Power Converter with Back Surface Reflector for Medical Applications. In Proceedings of the 2021 IEEE 48th Photovoltaic Specialists Conference (PVSC), Fort Lauderdale, FL, USA, 20–25 June 2021; pp. 1954–1959.
62. France, R.M.; Hinojosa, M.; Ahrenkiel, S.P.; Young, M.R.; Johnston, S.W.; Guthrey, H.L.; Steiner, M.A.; Geisz, J.F. Improvement of front-junction GaInP by point-defect injection and annealing. In Proceedings of the 2021 IEEE 48th Photovoltaic Specialists Conference (PVSC), Fort Lauderdale, FL, USA, 20–25 June 2021; p. 2522.
63. Geisz, J.F.; Buencuerpo, J.; McMahon, W.E.; Klein, T.R.; Tamboli, A.C.; Warren, E.L. Fabrication, Measurement, and Modeling of GaInP/GaAs Three-Terminal Cells and Strings. In Proceedings of the 2021 IEEE 48th Photovoltaic Specialists Conference (PVSC), Fort Lauderdale, FL, USA, 20–25 June 2021; pp. 0154–0157.
64. Yamaguchi, M.; Dimroth, F.; Geisz, J.F.; Ekins-Daukes, N.J. Multi-junction solar cells paving the way for super high-efficiency. *J. Appl. Phys.* **2021**, *129*, 240901. [CrossRef]
65. Kimovec, R.; Helmers, H.; Bett, A.W.; Topič, M. Comprehensive electrical loss analysis of monolithic interconnected multi-segment laser power converters. *Prog. Photovolt. Res. Appl.* **2019**, *27*, 199–209. [CrossRef]
66. Kimovec, R.; Helmers, H.; Bett, A.W.; Topic, M. On the Influence of the Photo-Induced Leakage Current in Monolithically Interconnected Modules. *IEEE J. Photovolt.* **2018**, *8*, 541–546. [CrossRef]
67. Čičić, S.; Tomić, S. Automated design of multi junction solar cells by genetic approach: Reaching the >50% efficiency target. *Sol. Energy Mater. Sol. Cells* **2018**, *181*, 30–37. [CrossRef]
68. Algora, C.; García, I.; Delgado, M.; Peña, R.; Vázquez, C.; Hinojosa, M.; Rey-Stolle, I. Beaming power: Photovoltaic laser power converters for power-by-light. *Joule* **2022**, *6*, 340. [CrossRef]
69. Matsuura, M.; Nomoto, H.; Mamiya, H.; Higuchi, T.; Masson, D.; Fafard, S. Over 40-W Electric Power and Optical Data Transmission Using an Optical Fiber. *IEEE Trans. Power Electron.* **2020**, *36*, 4532. [CrossRef]
70. Helmers, H.; Armbruster, C.; von Ravenstein, M.; Derix, D.; Schoner, C. 6-W Optical Power Link With Integrated Optical Data Transmission. *IEEE Trans. Power Electron.* **2020**, *35*, 7904. [CrossRef]

71. Jaffe, P. Practical power beaming gets real. *IEEE Spectrum*. 21 May 2022. Available online: https://spectrum.ieee.org/power-beaming (accessed on 15 June 2022).
72. Wilkins, M.M.; Ishigaki, M.; Provost, P.-O.; Masson, D.; Fafard, S.; Valdivia, C.E.; DeDe, E.M.; Hinzer, K. Ripple-Free Boost-Mode Power Supply Using Photonic Power Conversion. *IEEE Trans. Power Electron.* **2018**, *34*, 1054–1064. [CrossRef]
73. Sweeney, S.J. Optical wireless power at eye-safe wavelengths: Challenges and opportunities. In Proceedings of the 3rd Optical Wireless and Fiber Power Transmission Conference (OWPT2021), Yokohama, Japan, 19–22 April 2021.
74. Wong, Y.L.; Shibui, S.; Koga, M.; Hayashi, S.; Uchida, S. Optical Wireless Power Transmission Using a GaInP Power Converter Cell under High-Power 635 nm Laser Irradiation of 53.5 W/cm^2. *Energies* **2022**, *15*, 3690. [CrossRef]
75. Kalyuzhnyy, N.A.; Emelyanov, V.M.; Evstropov, V.V.; Mintairov, S.A.; Mintairov, M.A.; Nahimovich, M.V.; Salii, R.A.; Shvarts, M.Z. Optimization of photoelectric parameters of InGaAs metamorphic laser (λ = 1064 nm) power converters with over 50% efficiency. *Sol. Energy Mater. Sol. Cells* **2020**, *217*, 110710. [CrossRef]
76. TYi-Chen, Z.; Hai-Yang, Z.; Zhang, H.-Y.; Zhao, C.-M.; Zhang, Y.-C.; Xu, P.; Muñoz, M. High-Power High-Efficiency Laser Power Transmission at 100 m Using Optimized Multi-Cell GaAs Converter. *Chin. Phys. Lett.* **2014**, *31*, 104203.
77. Khvostikov, V.P.; Kalyuzhnyy, N.A.; Mintairov, S.A.; Potapovich, N.S.; Sorokina, S.V.; Shvarts, M.Z. Module of Laser-Radiation (λ = 1064 nm) Photovoltaic Converters. *Semiconductors* **2019**, *53*, 1110–1113. [CrossRef]
78. Guan, C.; Li, L.; Ji, H.-M.; Luo, S.; Xu, P.; Gao, Q.; Lv, H.; Liu, W. Fabrication and Characterization of a High-Power Assembly with a 20-Junction Monolithically Stacked Laser Power Converter. *IEEE J. Photovolt.* **2018**, *8*, 1355–1362. [CrossRef]
79. Proulx, F.; York, M.C.A.; Provost, P.O.; Arès, R.; Aimez, V.; Masson, D.P.; Fafard, S. Measurement of strong photon recycling in ultra-thin GaAs n/p junctions monolithically integrated in high-photovoltage vertical epitaxial heterostructure architec-tures with conversion efficiencies exceeding 60%. *Phys. Status Solidi RRL* **2017**, *11*, 1600385. [CrossRef]
80. Wilkins, M.; Valdivia, C.E.; Gabr, A.M.; Masson, D.; Fafard, S.; Hinzer, K. Luminescent coupling in planar opto-electronic de-vices. *J. Appl. Phys.* **2015**, *118*, 143102. [CrossRef]
81. Lopez, E.; Höhn, O.; Schauerte, M.; Lackner, D.; Schachtner, M.; Reichmuth, S.K.; Helmers, H. Experimental coupling process efficiency and benefits of back surface reflectors in photovoltaic multi-junction photonic power converters. *Prog. Photovolt. Res. Appl.* **2021**, *29*, 461–470. [CrossRef]
82. Xia, D.; Krich, J.J. Efficiency increase in multijunction monochromatic photovoltaic devices due to luminescent coupling. *J. Appl. Phys.* **2020**, *128*, 013101. [CrossRef]
83. Hwang, S.; Shim, J.; Eo, Y. Ohmic Contacts of Pd/Zn/M(=Pd or Pt)/Au to p-Type InP. *J. Korean Phys. Soc.* **2005**, *46*, 751.
84. Laser Model KE70HA5FA from BWT Beijing Ltd. Was Used as the ~1470 nm Source. Available online: https://www.bwt-bj.com/en/product/ (accessed on 15 June 2022).